Available online at www.sciencedirect.com
SCIENCE DIRECT®
PERGAMON
Polyhedron 22 (2003) 2689–2697
POLYHEDRON
www.elsevier.com/locate/poly

Synthesis, structural investigations and magnetic properties of dipyridinated manganese phthalocyanine, $MnPc(py)_2$

Jan Janczak [a,*], Ryszard Kubiak [a], Małgorzata Śledź [a], Horst Borrmann [b], Yuri Grin [b]

[a] *W. Trzebiatowski Institute of Low Temperature and Structure Research, Polish Academy of Sciences, Okólna 2 str., P.O. Box 1410, 50-950 Wrocław, Poland*
[b] *Max-Planck Institut für Chemische Physik Fester Stoffe, Notnizer str. 40, D1187 Dresden, Germany*

Received 23 March 2003; accepted 22 May 2003

Abstract

The $MnPc(py)_2$ complex was obtained in the reaction of MnPc with purified and dry pyridine under non-oxidation conditions. It crystallises in the centrosymmetric space group $P2_1/c$ of the monoclinic system with two molecules per unit cell. The Mn^{2+} cation is coordinated by four *N*-isoindole atoms of phthalocyaninato(2−) macrocycle and axially by two nitrogen atoms of pyridine molecules into a tetragonal bipyramid. The $MnPc(py)_2$ crystals are moderately stable under air, but in pyridine solution the $MnPc(py)_2$ complex undergoes oxidation by O_2 yieldings the binuclear manganese(III) μ-oxo complex $(MnPcpy)_2O$ as evidenced by the UV–Vis spectroscopy. The magnetic susceptibility measurement performed on solid sample of $MnPc(py)_2$ shows the Curie–Weiss behaviour in the temperature region of 300–15 K. The calculated magnetic moment μ_{eff} indicates three unpaired electrons ($S = 3/2$), thus the ground state configuration of Mn ion is $(a_{1g})^2(e_g)^2(b_{2g})^1$, and the $MnPc(py)_2$ complex is the intermediate spin complex. Below 5.5 K (T_N) the magnetic susceptibility sharply decreases due to the cooperative intermolecular antiferromagnetic interactions.

Keywords: Dipyridinated manganese(II) phthalocyanine; Crystal structures; Magnetic properties; Antiferromagnetic interactions; Oxidation; UV–Vis spectroscopy

1. Introduction

The ability of the metal(II) phthalocyanines to coordinate additional N- or O-donor ligands or solvent molecules with formation of the 4+1 and 4+2 coordinated complexes is well known [1–8]. The formation of metallophthalocyaninato complexes with pyridine depends strongly on the electronic configuration of the central metal ion. The metallophthalocyanine molecule, as an acceptor, and pyridine molecule with the lone electron pair on N atom, as a donor, could attract each other through donor–acceptor interactions, however the composition of the formed products is very sensitive to the processing conditions. Lever was the first to report the existence of the pyridine complexes in solution for MgPc, FePc and for MnPc [9]. Moreover, later it has been stated that the MnPc is able to form a stable pyridine complex only in an oxidative form [10] and the μ-oxo-bis(phthalocyaninato(2−)) manganese(III) complex with the composition of $(MnPc(py))_2O$ has been isolated and structurally characterized by X-ray diffraction technique [11]. However, we suppose that the formation of the MnPc complex with pyridine without oxygen as a bridging atom could be also possible. The existence of the six-coordinated complex of iron(II) phthalocyanine with 4-methylpyridine has also been reported [12]. Later this bis(4-methylpyridine)-phthalocyaninato(2−) iron(II) complex has been structurally characterized [13]. Subsequently the five- and six-coordinated complexes of CoPc with pyridine, CoPc(py) and $CoPc(py)_2$, have been reported [14], however, well-characterized solid state compound as single crystal has been described only on the six-coordinated $CoPc(py)_2$ complex [15]. In addition it has been reported that zinc phthalocyanine forms some complexes with various amines [16], and one of them, the zinc phthalocyanine

* Corresponding author. Tel.: +48-71-343-5021; fax: +48-71-344-1029.
E-mail address: janczak@int.pan.wroc.pl (J. Janczak).

0277-5387/03/$ - see front matter © 2003 Elsevier Ltd. All rights reserved.
doi:10.1016/S0277-5387(03)00361-9

with *n*-hexylamine has been characterized by the single crystal X-ray diffraction [17].

In the course of our investigations of the metal(II) phthalocyanines in pyridine solution, quite recently, we have obtained the dipyridinated magnesium, cobalt and iron phthalocyanines, $MgPc(py)_2$, $CoPc(py)_2$ and $FePc(py)_2$, in crystalline form [15,18]. Additionally, we have stated that the crystals of $MgPc(py)_2$ are stable under dry atmosphere only, while under moist air this complex interacts with water molecules and converts into $MgPc(H_2O)\cdot 2py$, which has been previously structurally characterized [19]. Besides this $MgPc(H_2O)\cdot 2py$ complex, quite recently, it has been reported that during recrystallization of MgPc from pyridine solution, besides the $MgPc(H_2O)\cdot 2py$, other crystals with the composition of $2(MgPc(H_2O)\cdot 3py$ have been obtained [20]. The Co and Fe dipyridinated phthalocyaninato complexes are the low-spin complexes [15]. Our investigations of $MgPc(py)_2$, $CoPc(py)_2$ and $FePc(py)_2$ shown that the Fe-complex is the most stable and Co-complex the least stable within these complexes. Additionally, we have no evidence on the formation of the 1:1 complexes (M(II):py) by the thermal dissociation as was suggested earlier for the CoPc complex with pyridine [14].

The phthalocyaninato complexes of manganese are of peculiar interest because they open up the possibility of their utilisation as sensors and are important in the field of biological oxidative processes, coordination chemistry and catalysis [21]. They are also promising as organometallic magnetic materials [22]. It has been also shown by Miller [23], that the metallophthalocyanine analogue, the manganese porphyrin with tetracyanoethylene complex, displays ferromagnetism. Those circumstances were the reasons for the presented study, and here we report the results.

Our aim of the present study was to obtain the manganese(II) dipyridinated phthalocyaninato complex in crystalline form and the information concerning its stability and the transformation processes in the oxidative conditions. Subsequently, to extend the information about the stereochemistry and the properties of the M–N(py) coordination bond we compare the crystal structure of $MnPc(py)_2$ with the previously described complexes of $MgPc(py)_2$, $CoPc(py)_2$ and $FePc(py)_2$ [15,18].

2. Experimental

2.1. Synthesis

The substrates i.e. MnPc and pyridine were purchased from Sigma-Aldrich. The microcrystalline powder of MnPc (0.4 g) and purified and dry pyridine (10 ml), were placed into a glass ampoule and next degassed and sealed under vacuum. Than the mixture was allowed to react at 433 K for 1 day. After that, the solid part was removed from the mother liquor by filtration and the well formed, parallelepiped violet crystals of a various sizes, but identical in colour and shape, were selected. *Anal*. Found: Mn, 7.65; C, 69.42; H, 3.52; N, 19.41% indicating the composition $MnPc(py)_2$; calculated values for $Mn(C_{32}H_{16}N_8)(C_5H_4N)_2$: Mn, 7.57; C, 69.52; H, 3.61 and N, 19.30. It should be added that the filtrate was evaporated to dryness at room temperature. The precipitated solid substance was examined by X-ray powder diffraction on a STOE powder diffractometer with linear PSD detector. The powder diffraction pattern was identical with the pattern of the starting MnPc material.

2.2. Thermal measurements

Thermal analysis was carried out on a Lineis L81 thermobalance apparatus with Pt crucibles. The powdered Al_2O_3 has been used as a standard reference. The measurements were performed on samples of 15–20 mg under static air atmosphere on heating from room temperature to about 280 °C with the heating rate of 5 °C min^{-1}.

2.3. X-ray single crystal measurement

Data collection was carried out on a KUMA KM-4 diffractometer with a two-dimensional area CCD detector. The graphite monochromatized Mo Kα radiation ($\lambda = 0.71073$ Å) and ω-scan technique with $\Delta\omega = 0.75^\circ$ for one image were used for data collection. The 960 images for six different runs covering over 95% of the Ewald sphere were performed. One image as a standard was used for monitoring the stability of the intensities after every 40 images. Integration of the intensities, corrections for Lorenz and polarization effects were made using a KUMA KM-4 CCD program package [24]. The face-indexed analytical absorption was calculated using the SHELXTL program [25]; max. and min. transmission factors being 0.956 and 0.869. 4510 independent reflections (a total of 18 779 reflections were integrated, $R_{int} = 0.0373$) were used for crystal structure solution and refinement. The structure was solved by Patterson method. The hydrogen atoms of the phenyl rings were located from the $\Delta\rho$ maps, but in the final refinement their positions were constrained using HFIX 43 with the isotropic thermal parameters of $1.2U_{eq}$ of the carbon atoms linked directly to the H atoms. The structure was refined with anisotropic thermal parameters for all non-hydrogen atoms by full-matrix least-squares methods using SHELXL-97 program [26]. The final difference map calculation showed no peaks of chemical significance; the largest were +0.335 and −0.377 e $Å^{-3}$. More details of the data collection parameters and the final agreement factors are collected

Table 1
Crystal data and structure refinement for $MnPc(py)_2$

Chemical formula	$C_{42}H_{26}N_{10}Mn$
Formula weight	725.67
Temperature (K)	295(2)
Wavelength (Å)	0.71073
Crystal system	monoclinic
Space group	$P2_1/c$
Unit cell dimensions	
a (Å)	9.650(2)
b (Å)	19.958(4)
c (Å)	9.171(2)
β (°)	111.66(3)
V (Å^3)	1641.6(6)
Z	2
D_{calc} (Mg m^{-3})	1.468, 1.46
Absorption coefficient (mm^{-1})	0.453
Crystal size (mm)	0.32 × 0.18 × 0.10
ϑ_{max} for data collection	29.85
Limiting indices	$-12 \le h \le 12$
	$-25 \le k \le 27$
	$-10 \le l \le 12$
Reflections collected/unique/observed	18 779/4510/3211
$[F^2 > 2\sigma(F^2)]$	$[R_{int} = 0.0373]$
Refinement method	full-matrix least-squares on F^2
Data/restraints/parameters	4510/0/242
Goodness-of-fit on F^2	1.018
Final R [a] indices $[I > 2\sigma(I)]$	0.0455
wR [b] indices (all data)	0.1142
Largest peak and hole on Δ map (e Å^{-3})	0.335 and −0.377

[a] $R = \Sigma||F_o|-|F_c||/\Sigma F_o$.
[b] $wR = \{\Sigma[w(F_o^2-F_c^2)^2]/\Sigma wF_o^4\}^{1/2}$; $w^{-1} = [\sigma^2(F_o^2)+(0.0481P)^2+0.7299P]$ where $P = (F_o^2+2F_c^2)/3$.

in Table 1. Selected bond lengths and angles are listed in Table 2.

2.4. Magnetic susceptibility measurements

The temperature dependence of the magnetic susceptibility of $MnPc(py)_2$ was recorded from 300 to 1.8 K on Quantum Design SQUID magnetometer (San Diego, CA) on the sample of 115 mg. The magnetization on magnetic field dependence was recorded from 0 to 5 T at 1.9 K.

2.5. Spectroscopic measurements

Measurements of the electronic spectra were carried out at room temperature using a Varian Cary 5E UV–VIS–NIR spectrometer. The UV–Vis spectra were recorded from pyridine solution in 0.5-cm quartz cell.

3. Results and discussion

3.1. Synthesis and characterization

The preparation method of the single crystal of the dipyridinated manganese(II) phthalocyaninato(2−) complex, $MnPc(py)_2$, is very fast and simple. A suspension of β-MnPc in purified and degassed pyridine was heated at 160 °C for 1 day. During the heating process in non-oxidation conditions the molecule of MnPc interacts by its positively polarized metal atom with the lone electron pair of nitrogen atom of pyridine molecules. As a result of this interaction the dipyridinated manganese(II) phthalocyaninato complex is formed. The obtained crystals of $MnPc(py)_2$ are moderately stable under air condition, but in pyridine solution the $MnPc(py)_2$ molecules interact with the oxygen and transform into the known μ-oxo-bis[phthalocyaninato(2−)]manganese(III) complex [11] as a result of the oxidation of $MnPc(py)_2$ complex by oxygen. The crystals of $MnPc(py)_2$ are soluble in pyridine, DMF, DMSO and other N- and O-donor solvents. The two other dipyridinated Fe and Co complexes $FePc(py)_2$ and $CoPc(py)_2$ are significantly more stable in air than this $MnPc(py)_2$ complex, are stable significantly under air condition [15], whereas the third known dipyridinated complex—$MgPc(py)_2$ is less stable under moist atmosphere [18]. The $MgPc(py)_2$ interacts with a water molecule and transforms into aqua complex with the composition of $(MgPcH_2O)\cdot 2py$ [18], in which the water molecule is coordinated directly to the central magnesium cation and pyridine molecules as acceptors are joined to the $MgPc(H_2O)$ molecule by the O–H···N(py) hydrogen bonds [19]. The contact of $MnPc(py)_2$ with non-oxidising dilute acid lead to the demetallation, leads metal-free phthalocyanine in the α-form [27].

Table 2
Comparison of the coordination of the central metal ion in dipyridinated phthalocyaninato(2−) complexes

Compound	$MnPc(py)_2$	MnPc	$FePc(py)_2$	FePc	$CoPc(py)_2$	CoPc	$MgPc(py)_2$	MgPc
M–N_{iso} (Å)	1.954(2)	1.933(4)	1.938(2)	1.926(2)	1.930(2)	1.908(3)	2.006(2)	2.011(3)
M–N(py) (Å)	2.114(2)		2.039(2)		2.340(2)		2.376(2)	
Rotation angle (°)	34.5(2)		36.1(2)		28.6(2)		26.6(2)	
C–N_{iso} (Å)	1.382(2)	1.394(8)	1.377(5)	1.378(3)	1.376(2)	1.368(4)	1.367(2)	1.376(2)
C–N_{aza} (Å)	1.330(2)	1.317(8)	1.328(4)	1.323(3)	1.329(2)	1.318(4)	1.343(2)	1.334(2)
Reference	This work	[28]	[15]	[29]	[15]	[29]	[18]	[30]

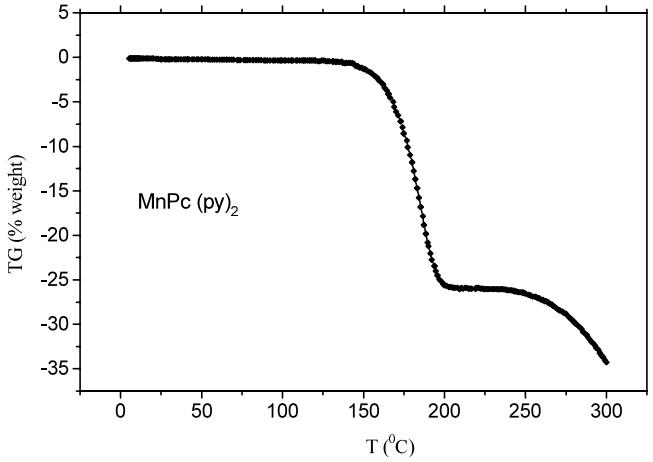

Fig. 1. Thermogram of the solid state sample of $MnPc(py)_2$.

As can be seen from the thermogram (Fig. 1) the $MnPc(py)_2$ complex is stable up to about 180 °C. Above this temperature two axial equivalent Mn–N(py) bonds break simultaneously giving MnPc in powdered form. The X-ray powder diffraction pattern indicates the β-modification. The thermogravimetric analysis gives no evidence on the formation of the 1:1 adduct (MnPc:py) by the thermal dissociation. The axial M–N(py) bonds in $MnPc(py)_2$ complex are stronger than the corresponding ones in $CoPc(py)_2$ (both Co–N(py) bonds break at ~140 °C) and weaker than in the $FePc(py)_2$ (both Fe–N(py) bonds break at ~225 °C) [15]. Above 250 °C the sublimation process of MnPc begins (see Fig. 1).

3.2. Description of the structure

The molecular structure of the dipyridinated phthalocyaninato(2−) manganese(II) complex is illustrated in Fig. 2. The manganese cation lies at the inversion center, thus the $MnPc(py)_2$ molecule is centrosymmetric. The coordination polyhedron around the central Mn ion approximates to a tetragonal bipyramid. The central metal ion (Mn^{2+}) and the four isoindole nitrogen atoms of the phthalocyaninato(2−) macrocycle lie on a plane. The pyridine molecules are coordinated by their lone electron pair at the nitrogen atoms to the central Mn atom in the axial positions. The orientation of the axially coordinated pyridine in relation to the phthalocyaninato macrocyclic ring is well described by the torsion angle of N3–Mn–N5–C17. The rotation of the pyridine molecule around the Mn–N5 axis would reduce the steric effect; i.e. the non-bonding distances between the ortho-hydrogen atoms of the axial pyridine ligand and the atoms of phthalocyaninato ring. In particular, if the rotation angle is equal to 0, the plane of pyridine ring is parallel to the Mn–N3 bond, or at the equivalent position rotated by 90°, the pyridine molecule is parallel to the Mn–N1 bond, making the non-bonding C···H distances greater than 2.5 Å. The second orientation, with the rotation angle of 45°, makes the axial pyridine plane parallel to the Mn–N(azamethine) axis and this orientation reduces the non-bonding distances between the ortho-H atoms of pyridine and the azamethine nitrogen atoms of phthalocyaninato(2−) macrocycle. Such conformation of $MnPc(py)_2$ complex is the most stable due to the greatest interaction (attractive forces) between the ortho-hydrogen atoms of pyridine molecules and the azamethine nitrogen atoms. However, the intermolecular interactions and the crystal packing forces present in the crystal make the rotation angle of the axial pyridine molecule plane 34.5(2)°. This angle is comparable to that observed in $FePc(py)_2$ (36.1(2)°) [15] and is greater than in $CoPc(py)_2$ (28.6(2)°) [15] and in $MgPc(py)_2$ (26.6(2)°) [18]. The main difference between the $MnPc(py)_2$ and other dipyridinated phthalocyaninato(2−) complexes is found in the axial M–N(py) coordination bond distances. The coordination geometries of the central metal ions in the dipyridinated complexes are collected in Table 3, which also contains the parameters of non-ligated M(II)Pc complexes, MnPc [28], FePc [29] and MgPc [30]. The M–N(py) axial bond in $MnPc(py)_2$ with a distance of 2.114(2) Å is longer than corresponding one in $FePc(py)_2$, but shorter than in $CoPc(py)_2$ [15] (see Table 3). The long M–N(py) axial bond distance in $CoPc(py)_2$ is likely due to the unpaired electron, which is essentially localised on the d_z^2 orbital of the Co^{2+}, thus the ground state configuration of the $CoPc(py)_2$ can be expressed as $(e_g)^4(b_{2g})^2(a_{1g})^1$ in accordance to the EPR and magnetic measurements [15]. The lengthening of the axial Co(II)–N(py) bond by about 0.3 Å in $CoPc(py)_2$ is supported by the molecular orbital calculation performed by Little and Ibers that gave a value of 2.05 Å for Co(III)–N(sp^2) bond (in the absence of the electron localization on the d_z^2 orbital)

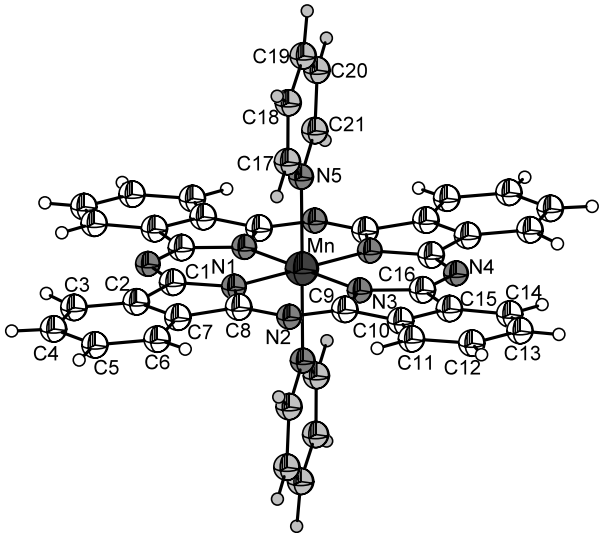

Fig. 2. View of the $MnPc(py)_2$ molecule with labeling scheme. Displacement ellipsoids are shown at the 50% probability level.

Table 3
Selected bond lengths (Å) and angles (°) for $MnPc(py)_2$

Bond lengths			
Mn–N1	1.953(2)		
Mn–N3	1.955(2)		
Mn–N5	2.115(2)		
C–N(pyrrole)		C–N(azamethine)	
C1–N1	1.382(2)	C8–N2	1.336(2)
C8–N1	1.381(2)	C9–N2	1.329(2)
C9–N3	1.382(2)	C16–N4	1.327(2)
C16–N3	1.383(2)	$C1^{i}$–N4	1.327(2)
Bond angles			
N1–Mn–N3	90.08(6)		
$N1^{i}$–Mn–N3	89.92(6)		
N1–Mn–N5	90.67(6)		
N3–Mn–N5	89.72(6)		

Symmetry code: $i = -x, -y, -z$.

[31]. The shorter Fe–N(py) bond distance in $FePc(py)_2$ is in agreement with the EPR measurement results ($FePc(py)_2$ is not EPR active) indicating that the $FePc(py)_2$ is the low-spin complex [15]. The ligation of FePc by two pyridine molecules leads to the change of the ground state from $(e_g)^3(b_{2g})^2(a_{1g})^1$ or $(e_g)^4(b_{2g})^1(a_{1g})^1$ in FePc [32,33] to the $(e_g)^4(b_{2g})^2$ in $FePc(py)_2$ [15]. In the present structure of $MnPc(py)_2$ complex the M–N(py) bond is intermediate between those found in iron and cobalt analogues (Table 3). This implicates the intermediate ground state $(a_{1g})^2(e_g)^2(b_{2g})^1$, with the localisation of the unpaired electron on d_z^2 orbital (more details in the next section). The values of the M–N(py) coordination bond distances in the dipyridinated phthalocyaninato(2−) complexes indicate on their strength and correlate well with the stability of these complexes. Among known dipyridinated transition metal complexes, $MnPc(py)_2$, $FePc(py)_2$ and $CoPc(py)_2$, the axial pyridine molecules are coordinated strongest in Fe-complex as shown the thermogravimetric analysis [15]. The dipyridinated Mn-complex is more stable than the Co analogue, this is likely due to the different ground state configuration of the central metal cation. A similar correlation between the short, in Pc-plane, and long, perpendicular to the Pc, M–N bond lengths is observed in cobalt(II) phthalocyaninato(2−) complex with axially coordinated 4-methylpyridine molecules [13] and in the isostructural crystal of $MgPc(py)_2$ [18]. The long M–N coordination bonds have also been observed in several axially coordinated porphyrinato magnesium complexes [34–37] and in axially coordinated porphyrinato cobalt(II) complexes [38].

The C–C and C–N bond lengths of the phthalocyaninato(2−) macrocycle in $MnPc(py)_2$ complex are normal and the values of the chemically equivalent bond lengths are not different from the corresponding values in several metallophthalocyaninato complexes, including metal-free phthalocyanine [27]. However, it should be noted that the good accuracy of the present structure determinations and relatively low standard deviations indicate the small differences between the average values of $C–N_{iso}$ and $C–N_{aza}$ bond lengths (see Table 3). These differences indicate an accumulation of the charge density on the outer carbon atoms of pyrrole rings as well as on the bridging azamethine nitrogen atoms of phthalocyaninato macrocycle. This can be explained by an important role of the electron back donation from the metal d(π) orbitals to the ligand $\pi^*(e_g)$ anti-bonding orbital, since the calculated maximum charge density is mainly located on those atoms [39–41]. The accumulation of the charge density on the outer carbon atoms of pyrrole rings and on the bridging azamethine nitrogen atoms has also been evidenced from the experimental density maps derived form the low temperature high resolution X-ray experiments [42–45].

The arrangement of $MnPc(py)_2$ molecules in the unit cell is illustrated in Fig. 3. The crystal is built up from isolated $MnPc(py)_2$ molecules that form alternating sheets, with molecules related by a screw axis and glide plane. Within one sheet the phthalocyaninato(2−) macrocycles are parallel to each other and between the sheets the phthalocyaninato(2−) planes are perpendicular. The neighbouring $MnPc(py)_2$ molecules within one sheet overlap by their two phenyl rings which are separated by ~3.15 Å. This value indicates the π–π interaction between these phenyl rings of the phthalocyaninato(2−) macrocycles within the sheet, since this distance is shorter than the van der Waals distance of ~3.4 Å for aromatic carbon atoms [46].

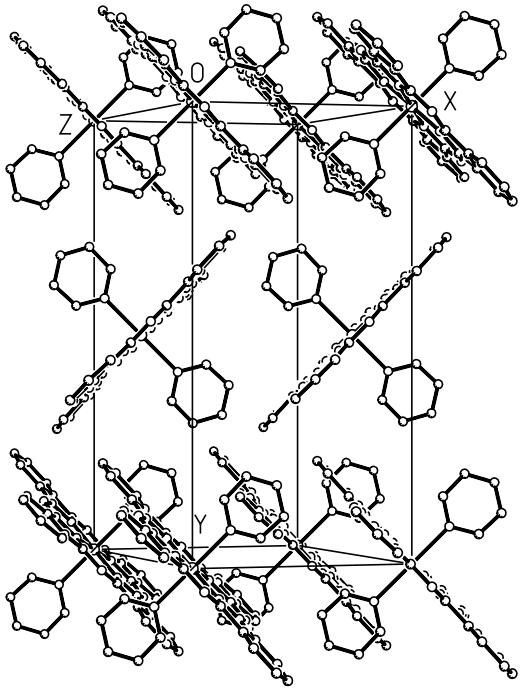

Fig. 3. Arrangement of the $MnPc(py)_2$ molecules in the unit cell.

3.3. UV–Vis spectroscopy

The UV–Vis spectroscopy was used for estimation of the stability of $MnPc(py)_2$ in pyridine solution as well as of the oxidation and reduction reactions of this complex. The electronic absorption spectrum of starting $MnPc(py)_2$ in pyridine solution is shown in Fig. 4 (solid line). This spectrum is quite similar to that reported for MnPc in pyridine solution [47], thus it should be stated that the pyridine molecules very easily coordinate to the MnPc even at room temperature with the formation of $MnPc(py)_2$ complex. However, this spectrum is different in comparison with the spectrum of MnPc obtained on the thin film of MnPc prepared by sublimation in vacuum [48] which shows the relatively broad Q band at $\sim$705 nm. In the spectrum of $MnPc(py)_2$ in pyridine solution the Q band is observed at 660 nm and corresponds to the excitation between the HOMO(a_{1u}) and LUMO (e_g) orbitals. Several theoretical calculations for the D_{4h} symmetry of the metallophthalocyaninato and metalloporpyrinato complexes predict five distinct bands (Q, B, N, L and C) in the spectral region of 200–800 nm [49]. In the spectrum of starting $MnPc(py)_2$ complex in pyridine solution the B band which is mostly an $a_{2u} \rightarrow e_g$ transition is observed at $\sim$360 nm. Both Q and B bands are characteristic for the phthalocyaninato(2−) macrocyclic ligand. The Q band in the spectrum of $MnPc(py)_2$ splits into two bands at $\sim$660 and $\sim$692 nm. The splitting of the Q band is characteristic and common feature for most metallophthalocyaninato complexes [50,51]. The splitting value is not too great and is likely due to the vibronic coupling in the excited state [52]. The N and L bands resulting mainly from contributions of $b_{2u} \rightarrow e_g$ and $a_{1u} \rightarrow e_g$ transitions [53–55] are observed at $\sim$328 and 307 nm, respectively. In summary, the spectrum of starting $MnPc(py)_2$ complex in pyridine solution in the absence of air has absorption peaks at 692, 660, 643, 605, 360, 328 and 305 nm (see Fig. 4, solid line). On exposure to air, the bands in the Q region decrease quickly with simultaneous increase of the bands in the B spectral region. Additionally, the new band appears at $\sim$620 nm that very quickly increases. This band is assigned to the transition in the dinuclear manganese(III) μ-oxo-complex, $(MnPcpy)_2O$, that is formed by oxidation of the $MnPc(py)_2$ by O_2 (see Scheme 1, complex III). This assignment is in agreement with the suggestion of Yamamoto et al. [48]. From the completely oxidised solution (the band at 620 nm, ε is twice that for the starting $MnPc(py)_2$ complex) a purple compound was obtained, which elemental analysis is in agreement with the dinuclear manganese(III) μ-oxo-complex (complex III, Scheme 1). Elvidge and Lever [56] studying the MnPc in a pyridine solution under exposure to air observed an absorption band at 712.5 nm. In this region we observed initially slight decreasing and next the increasing of the background. Finally after 75 h the band at $\sim$716 nm appeared. This band is characteristic for the hydroxopyridine phthalocyaninato manganese(III) complex (see Scheme 1, complex IV). This complex is formed by a hydrolysis of the dinuclear manganese(III) μ-oxo-complex. The MnPc(OH)(py) complex can be also obtained from the $MnPc(py)_2$ complex in solution of pyridine/H_2O under exposure to air. Our investigations clearly evidenced that the $MnPc(py)_2$ complex in dry pyridine and in the absence of air is stable (the characteristic band at 660 nm), but under exposure to air the very quick oxidation process

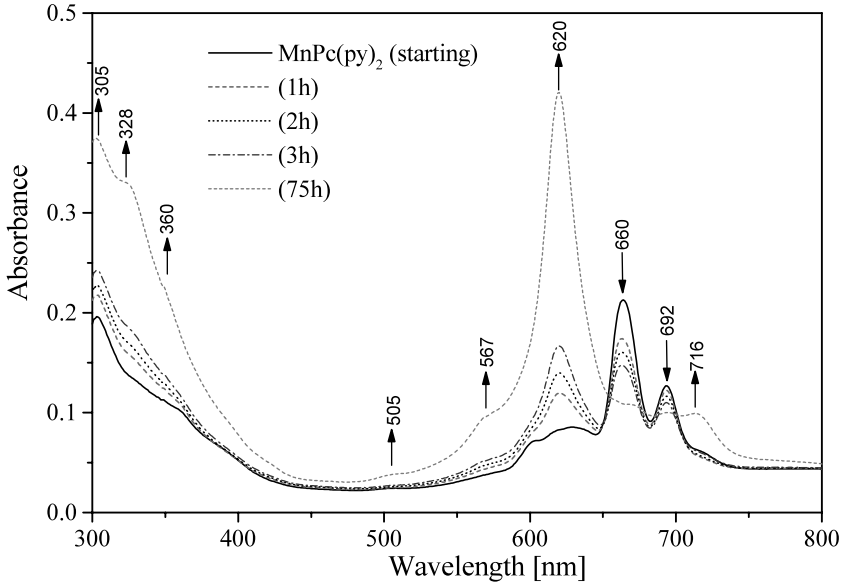

Fig. 4. Electronic absorption spectra of the starting $MnPc(py)_2$ complex in pyridine solution (solid line) and the oxidation products (dashed and dotted lines).

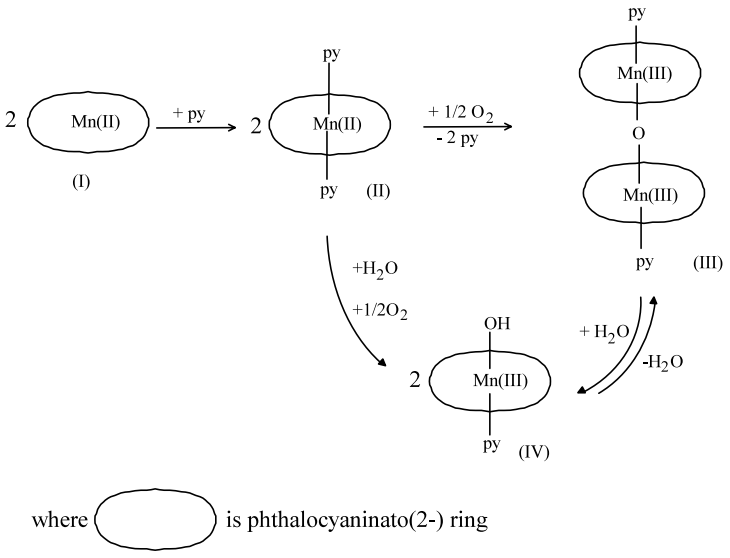

Scheme 1.

of $MnPc(py)_2$ to the dinuclear manganese(III) μ-oxo-complex, $(MnPcpy)_2O$ (the characteristic band at 620 nm) takes place, which is the most stable complex in the used conditions. In the spectrum of the starting $MnPc(py)_2$ complex in pyridine solution (solid line on the Fig. 4) at the region about 620 nm a weak broad band is observed, which indicates that during the preparation of the solution of $MnPc(py)_2$ in pyridine the oxidation process begins.

3.4. Magnetic properties

A plot of the reciprocal molar susceptibility versus temperature for $MnPc(py)_2$ complex is shown in Fig. 5. The corrections for diamagnetic susceptibility of the phthalocyaninato(2−) macrocycle (-290×10^{-6} cm^3 mol^{-1}) and pyridine molecules (44×10^{-6} cm^3 mol^{-1}) have been included to the molar susceptibility [57]. The experimental data in the region of 300–15 K are well approximated by a Curie–Weiss law with the value of $\Theta \cong -4.5$ K for the Curie constant. A temperature dependence of the effective magnetic moment down to 1.9 K is shown in Fig. 6. At room temperature the effective magnetic moment calculated for $MnPc(py)_2$ is $\mu_{eff} \cong 3.62\mu_B$ and it is constant from room temperature down to ~ 60 K. This value ($\mu_{eff} \cong 3.62\mu_B$) indicates the intermediate-spin $MnPc(py)_2$ complex with the three unpaired electrons per molecule arising from the ground state configuration of $(a_{1g})^2(e_g)^2(b_{2g})^1$. However, this value is slightly lower than the value of $3.88\mu_B$ calculated for the spin-only magnetic moment for $S = 3/2$. The slightly lower value of μ_{eff} than the calculated is likely due to the fact that the starting $MnPc(py)_2$ solid sample used for the magnetic measurement was not

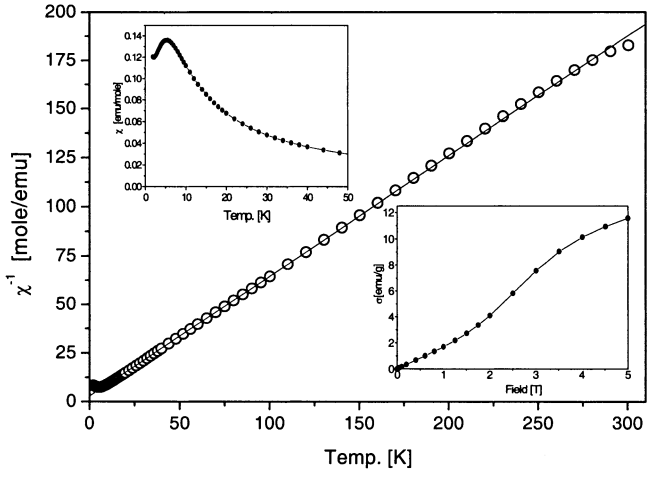

Fig. 5. Plots of the χ_M (insert top) and $1/\chi_M$ of the $MnPc(py)_2$ solid sample versus T and magnetization versus magnetic field strength (insert bottom).

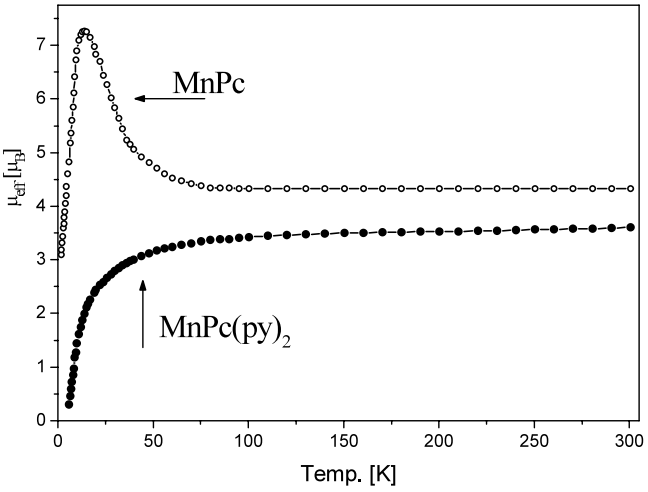

Fig. 6. Temperature dependence of magnetic moment of $MnPc(py)_2$ and MnPc for a comparison.

entirely pure, since the $MnPc(py)_2$ complex is moderately stable in air and some amount of dinuclear manganese(III) μ-oxo-complex, $(MnPcpy)_2O$, is present. This dinuclear manganese(III) μ-oxo-complex with four electrons on Mn^{3+} cation exhibits diamagnetic character due to the complete spin pairing which is unusual for this ion but is possible under two conditions: (1) antiferromagnetic interactions between oxygen-bridged manganese(III) ions that often occurs for μ-oxo-complexes of Mn(III) and (2) by pairing of the electrons on the d_{xz}, d_{yz} orbitals (e_g) that are the lowest lying of the manganese(III) d-orbitals as have been suggested by Yamamoto et al. [48].

The shape of the curve of the temperature dependence of magnetic susceptibility below 15 K down to the 1.9 K (the lowest temperature of the measurement) suggests the cooperative intermolecular antiferromagnetic interaction below $T_N \cong 5.5(2)$ K. The calculated magnetic moment at the lowest temperature (1.9 K) is $\mu_{eff} \cong 0.28\mu_B$. In the crystal of $MnPc(py)_2$ the distances of 9.171(2) and 10.982(2) Å between the magnetic Mn^{2+} ions in one sheet and between the sheets, respectively, are too large for a direct interaction of 3d-orbitals to contribute significantly to the magnetic exchange phenomenon. Thus, the possibility of spin–spin coupling between the magnetic centres (Mn^{2+} ions) via a superexchange mechanism, which involves the π electron system of the $MnPc(py)_2$ itself it should be considered. The distance of ~3.15 Å between adjacent and partially overlapped phthalocyaninato(2−) macrocycles within one sheet is sufficient to ensure the cooperative intermolecular interactions yielding the antiferromagnetic orientation of magnetic moments of neighbouring $MnPc(py)_2$ molecules within the sheet and quick decreasing of the μ_{eff}. The magnetic susceptibility of $MnPc(py)_2$ is independent of the magnetic field strength in the range of 300–15 K, but below 15 K the susceptibility depends on the magnetic field strength. The magnetization curve at the lowest temperature (1.9 K) versus magnetic field strength (0–5 T) is shown in Fig. 5. For a comparison, the effective magnetic moment, μ_{eff}, for non-ligated manganese(II) phthalocyaninato complex (MnPc) at room temperature is equal to $4.33\mu_B$ per one molecule [58,59], and is greater than spin-only magnetic moment for $S = 3/2$ ($3.88\mu_B$). The greater μ_{eff} for non-ligated manganese(II) phthalocyanine is likely due to a mixing of the ground state configuration of $(b_{2g})^2(e_g)^2(a_{1g})^1$ ($^4A_{2g}$) with the excited state of $(b_{2g})^1(e_g)^2(a_{1g})^1(b_{1g})^1$ (^4E_g) as well as by a standard perturbation treatment mixing into the ground term via spin–orbit coupling [59]. Additionally quite different temperature dependence of μ_{eff} for MnPc has been observed. With decreasing of the temperature from 300 K to 14 K the increasing of the effective magnetic moment from 4.33 to $7.30\mu_B$ was observed which was explained by the ferromagnetic interactions. Below 14 K the μ_{eff} for MnPc decreases to the value of $\sim 3.10\mu_B$.

4. Conclusions

The ligation of MnPc by pyridine with the formation of the 4+2 coordinated complex of $MnPc(py)_2$ takes place only under non-oxidation conditions and in purified and dry pyridine. The formed crystals of $MnPc(py)_2$ are moderately stable in air, but in pyridine solution under air condition the oxidation process of the $MnPc(py)_2$ complex by oxygen takes place rapidly and yields the dinuclear manganese(III) μ-oxo complex with the composition of $[MnPc(py)]_2O$. Under moist atmosphere or by adding a small amount of water the dinuclear manganese(III) μ-oxo complex undergoes hydrolysis with the formation of another manganese(III) complex—MnPc(OH)py. The ligation of the MnPc complex by pyridine changes its magnetic properties. The μ_{eff} of $MnPc(py)_2$ and MnPc are almost constant in the wide temperature range (300 to ~50 K). At lower temperatures the μ_{eff} of MnPc increases to the value of $7.30\mu_B$ at 14 K due to ferromagnetic interactions. Further decreasing of the temperature sharply decrease the μ_{eff} to the value of $3.10\mu_B$. The $MnPc(py)_2$ exhibits below 5.5 K (T_N) sharp decreases of magnetic susceptibility and μ_{eff} due to the cooperative antiferromagnetic interactions.

5. Supplementary materials

Details on data collection and refinement, fractional atomic coordinates, anisotropic displacement parameters and full list of bond lengths and angles in CIF format has been deposited at the Cambridge Crystallographic Data Centre, CCDC No. 206149. Copies of this information may be obtained free of charge from The Director, CCDC, 12 Union Road, Cambridge, CB2 1EZ, UK (fax: +44-1223-336033; email: deposit@ccdc.cam.ac.uk or www: http://www.ccdc.cam.ac.uk).

Acknowledgements

This work was supported by a grant (No. 3 T09A 180 19) from the Polish State Committee for Scientific Research.

References

[1] J.M. Assour, J. Am. Chem. Soc. 87 (1965) 4701.
[2] B. Stymne, F.X. Sauvage, G. Wettermark, Spectrochim. Acta A36 (1980) 397.

[3] V.N. Nemykin, N. Kobayashi, V.Y. Chernii, V.K. Belsky, Eur. J. Inorg. Chem. (2001) 733.
[4] A. Endo, S. Matsumoto, J. Mizuguchi, J. Phys. Chem. A103 (1999) 8193.
[5] S. Matsumoto, A. Endo, J. Mizuguchi, Z. Kristallogr. 215 (2000) 182.
[6] B.W. Dale, Trans. Faraday Soc. 65 (1969) 33.
[7] B.W. Dale, R.J.P. Williams, P.R. Edwards, C.E. Johnson, Trans. Faraday Soc. 64 (1968) 620.
[8] M.J. Stillman, A.J. Thomson, J. Chem. Soc., Faraday Trans. 2 (70) (1974) 790.
[9] A.B.P. Lever, Adv. Inorg. Chem. Radiochem. 7 (1965) 27.
[10] L.H. Vogt, A. Zalkin, D.H. Templeton, Science 151 (1966) 569.
[11] L.H. Vogt, A. Zalkin, D.H. Templeton, Inorg. Chem. 6 (1967) 1725.
[12] T. Kobayashi, F. Kurokawa, T. Ashida, N. Uyeda, E. Suito, J. Chem. Soc., chem. Cemmua. (1971) 1631.
[13] F. Cariati, F. Morazzoni, C. Busetto, J. Chem. Soc., Dalton Trans. 9 (1978) 1018.
[14] F. Cariati, F. Morazzoni, C. Busetto, J. Chem. Soc., Dalton Trans. 9 (1975) 556.
[15] J. Janczak, R. Kubiak, Inorg. Chim. Acta 342 (2003) 64.
[16] T. Kobayashi, N. Uyeda, E. Suito, J. Phys. Chem. 72 (1968) 2446.
[17] T. Kobayashi, T. Ashida, N. Uyeda, E. Suito, M. Kakudo, Bull. Chem. Soc. Jpn 44 (1971) 2446.
[18] J. Janczak, R. Kubiak, Polyhedron 21 (2002) 265.
[19] M.S. Fischer, D.H. Templeton, A. Zalkin, M. Calvin, J. Am. Chem. Soc. 93 (1971) 2622.
[20] J. Mizuguchi, M. Mochizuki, Z. Kristallogr. NCS 217 (2002) 244.
[21] (a) C.C. Leznoff, A.B. Lever, Phthalocyanines: Properties and Applications, vol. 1, VCH Publishers, New York, 1989;
(b) C.C. Leznoff, A.B. Lever, Phthalocyanines: Properties and Applications, vol. 2, VCH Publishers, New York, 1993;
(c) C.C. Leznoff, A.B. Lever, Phthalocyanines: Properties and Applications, vol. 3, VCH Publishers, New York, 1993;
(d) C.C. Leznoff, A.B. Lever, Phthalocyanines: Properties and Applications, vol. 4, VCH Publishers, New York, 1996.
[22] J.S. Miller, A.J. Epstein, Coord. Chem. Rev. 206–207 (2000) 651.
[23] J.S. Miller, Inorg. Chem. 39 (2000) 4392.
[24] KUMA Diffraction, KUMA KM-4 CCD program package, Ver. 163, 2000, Wroclaw, Poland.
[25] G.M. Sheldrick, SHELXTL Program, Siemens Analytical X-ray Instrument Inc, Madison WI, 1991.
[26] G.M. Sheldrick, SHELXL-97, Program for the Solution and Refinement of Crystal Structures, University of Göttingen, Göttingen, Germany, 1997.
[27] J. Janczak, Polish J. Chem. 74 (2000) 157.
[28] R. Mason, G.A. Williams, P.E. Fielding, J. Chem. Soc., Dalton Trans. (1979) 676.
[29] J.F. Kirner, W. Dow, W.R. Scheidt, Inorg. Chem. 15 (1976) 1685.
[30] J. Janczak, R. Kubiak, Polyhedron 20 (2001) 2901.
[31] R.G. Little, J.A. Ibers, J. Am. Chem. Soc. 96 (1974) 4440.
[32] B.W. Dale, R.J.P. Williams, C.E. Johnson, T.L. Throp, J. Chem. Phys. 49 (1968) 3441.
[33] C.G. Barraclough, R.L. Martin, S. Mitra, R.C. Sherwood, J. Chem. Phys. 53 (1970) 1643.
[34] J. Bonnett, B.M. Hursthone, K.M.A. Malik, B. Mateen, J. Chem. Soc., Perkin Trans. 2 (1977) 2072.
[35] V. McKee, C.C. Ong, G.A. Rodley, Inorg. Chem. 25 (1984) 4242.
[36] V. McKee, G.A. Rodley, Inorg. Chim. Acta 151 (1988) 233.
[37] M.P. Byrn, C.J. Curtis, Y. Hsion, S.I. Kahn, S.H. Tendick, A. Terzis, C.S. Stouse, J. Am. Chem. Soc. 115 (1993) 9480.
[38] W.R. Scheidt, J. Am. Chem. Soc. 96 (1974) 84.
[39] D.C. Grenoble, H.G. Drickamer, J. Chem. Phys. 55 (1971) 1624.
[40] P.S. Braterman, R.C. Davies, R.J.P. Williams, Adv. Chem. Phys. 7 (1964) 359.
[41] M.H. Whangbo, K.R. Stewart, Isr. J. Chem. 23 (1983) 133.
[42] P. Coppens, L. Liend, N.J. Zhu, J. Am. Chem. Soc. 105 (1983) 6173.
[43] A. Holladay, P. Leung, P. Coppens, Acta Crystallogr. A39 (1983) 377.
[44] C. Lecomte, R.H. Bleising, P. Coppens, J. Am. Chem. Soc. 108 (1986) 6942.
[45] N. Li, Z. Su, P. Coppens, J. Landrum, J. Am. Chem. Soc. 112 (1990) 7296.
[46] L. Pauling, The Nature of the Chemical Bond, Cornell University Press, Ithaca, NY, 1960, p. 262.
[47] G. Engelsema, A. Yamamoto, E. Markham, M. Calvin, J. Phys. Chem. 66 (1962) 2517.
[48] A. Yamamoto, L.K. Phillips, M. Calvin, Inorg. Chem. 7 (1968) 847.
[49] (a) M. Gouterman, G.H. Wagiere, L.C. Snycer, J. Mol. Spectrosc. 11 (1963) 108;
(b) S.C. Mathur, J. Chem. Phys. 45 (1968) 3470;
(c) M. Zerner, M. Gouterman, H. Kobayashi, Theor. Chim. Acta 6 (1966) 44;
(d) A.M. Schafer, M. Gouterman, E.R. Davidson, Theor. Chim. Acta 30 (1973) 9;
(e) L. Edwards, M. Gouterman, J. Mol. Spectrosc. 33 (1970) 292;
(f) M.G. Cory, H. Hirose, M.C. Zerner, Inorg. Chem. 34 (1995) 2969;
(g) M.S. Liao, S. Scheiner, J. Chem. Phys. 114 (2001) 9780.
[50] T. Nozawa, N. Kobayashi, H. Hatamato, M. Uyeda, M. Sugami, Biochim. Biophys. Acta 626 (1980) 282.
[51] T. Nykong, Z. Gasyna, M.J. Stillman, Inorg. Chem. 26 (1987) 1087.
[52] T.C. VanCott, J.L. Rose, G.M. Meisner, B.E. Williamson, A.S. Schrimp, M.E. Boyle, P.N. Schatz, J. Phys. Chem. 93 (1989) 2999.
[53] L.K. Lee, N.H. Sabelli, R.P. Leberton, J. Phys. Chem. 86 (1982) 3926.
[54] A. Henrikson, B. Roos, R. Sundon, Theor. Chim. Acta 27 (1972) 303.
[55] H. Shiari, H. Tsuiki, E. Masuda, T. Koyama, K. Hanabusa, N. Kobayashi, J. Phys. Chem. 95 (1991) 417.
[56] J.A. Elvidge, A.B.P. Lever, Proc. Chem. Soc. (1959) 195.
[57] R. Havemann, W. Haberditzl, K.H. Mader, Z. Phys. Chem. 218 (1961) 71.
[58] A.B.P. Lever, J. Chem. Soc. (London) (1965) 1821.
[59] C.G. Barraclough, R.L. Martin, S. Mitra, R.C. Sherwood, J. Chem. Phys. 53 (1970) 1638.